

Asteroid Confusions with Extremely Large Telescopes

Gy. M. Szabó, A. E. Simon

Received: date / Accepted: date

Abstract Asteroids can be considered as sources of contamination of point sources and also sources of confusion noise, depending whether their presence is detected in the image or their flux is under the detection limit. We estimate that at low ecliptic latitudes, $\approx 10,000$ – $20,000$ asteroids/sq. degree will be detected with an E-ELT like telescope, while by the end of Spitzer and Herschel missions, infrared space observatories will provide $\approx 100,000$ serendipitous asteroid detections. The detection and identification of asteroids is therefore an important step in survey astronomy.

Keywords Solar System: minor planets, asteroids · Astronomical Data Bases: catalogs · Sources: infrared: Solar System

1 Introduction

The presence of asteroids has been recognized to be a significant source of confusion noise and contaminating point sources in images (e.g. Ivezić et al. 2001, Tedesco & Desert 2002; Meadows et al. 2004, Kiss et al. 2006, 2008). This confusion is most prominent in visible and infrared wavelengths, because asteroids reflect the sunlight in the visible, and have maximal thermal emission around 5 – $20 \mu\text{m}$. As sky surveys go deeper, the number of detected asteroids increases rapidly, and so do the number of asteroids near the detection limit. In this paper we examine how the presence of asteroids deteriorate the quality of data in sky survey images. We concentrate on three kinds of confusion: by undetected asteroids, by unrecognized asteroids and by identified asteroids. The following types of contaminations will be discussed in this paper:

- By undetected asteroids. The faint asteroid tracks contaminate the star field, and covering a non-negligible fraction of the field they contaminate the precise photometry. They must be considered as sources of confusion noise.
- By detected sources not recognized as asteroids. They essentially contaminate the star field, leading to potential false candidates for transient objects, variable stars,

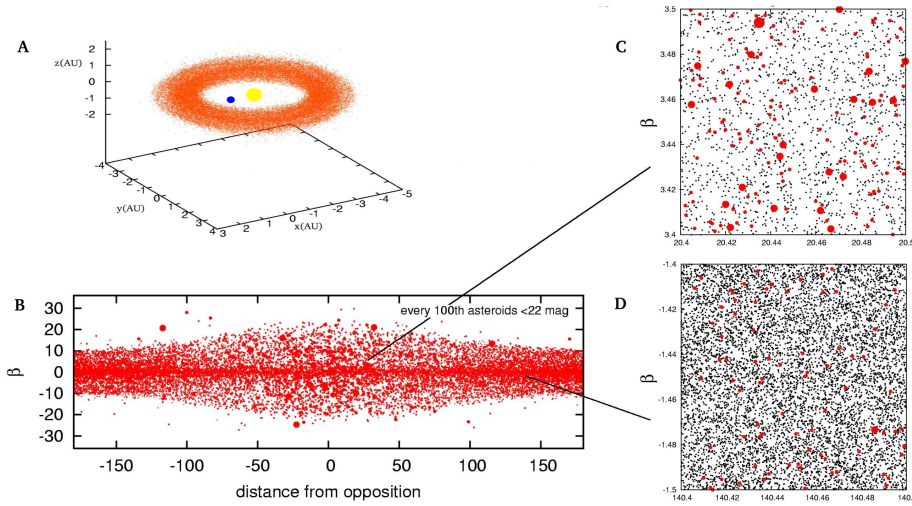


Fig. 1 The Solar System on 11 Sept. 2008. A: Space distribution of Statistical Asteroid Model (SAM, every 30th asteroids are plotted), in yellow and blue are the Sun and Earth. B: Distribution of asteroids <22 mag in the sky (every 100th asteroids are plotted). C and D: Simulated ELT images with 1-min exposure taken at different ecliptical coordinates, (see the ecliptical coordinates of the areas on the axis labels) showing detected asteroids (<25 mag; red dots) and undetected/trailed asteroids (black dots).

supernovae, GRB counterparts etc. They especially contaminate the very automated measuring pipelines.

- By asteroids recognized as asteroids. They do not bother much unless they are blend with objects of interest.

2 Estimating asteroid confusion in IR and visual wavelengths

Asteroids cause confusion because of the electromagnetic radiation they reflect and emit. The IR thermal emission is related to the mean surface temperature, the geometric albedo, the thermal inertia and the visible cross section. Via the thermal inertia and thermal conductivity, the shape has also slight influence on the infrared flux. In the visual, we observe reflected light. This is a product of the visible cross section and the geometric albedo, scaled by a factor depending on the configuration geometry (distances and the phase angle of the asteroid). In case of multicolor photometry, the knowledge of spectral albedo distribution is also necessary to predict the fluxes in each photometric bands. Thus, for all confusion estimates, a necessary input is the size distribution function (SDF) of asteroids in the Solar System. Determining the SDF is a non-trivial problem while the high complexity of this challenge has been recognized recently (Parker et al. 2008). An approximate solution is to choose a global SDF for all asteroids. The most widespread model SDF for asteroids is the Statistical Asteroid Model, SAM by Tedesco et al. (2005), which extends the empirical global SDF of known asteroids into the >1 km range.

On the other hand, ELTs will observe much smaller asteroids than the size limit of the SAM, and they will extend the detection limit to the 10 m – 100 m size range.

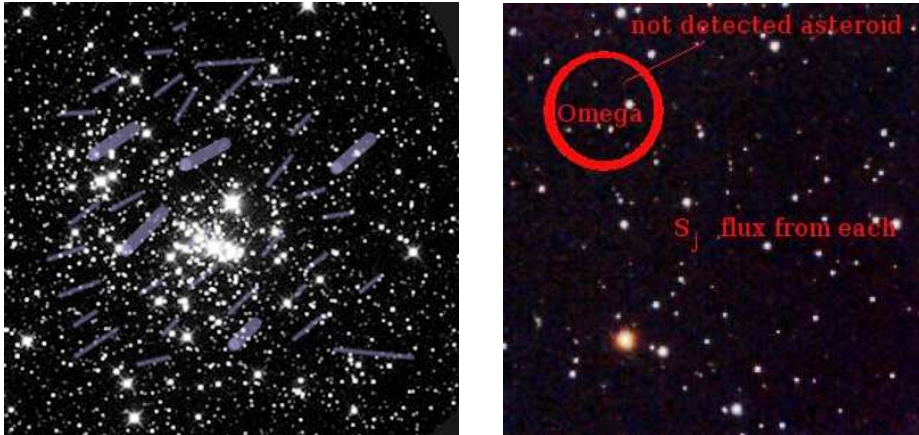


Fig. 2 Illustrations of confusion from undetected asteroids. Left panel: the moving faint asteroids appear as faint “noisy” trails in the background, leading to confusion noise. The trails are 1–1.5 arcs/min long for typical main belt asteroids in opposition. Right panel: the confusion noise is caused by the varying number of asteroid in counting cell of a fixed size.

A 1-minute exposure with a 25 m-class telescope enables us to do photometry of a 25 magnitude star with $S/N \approx 100$ quality. The complete discussion of asteroid confusions needs extending the asteroid brightness distribution model to < 30 magnitude (i.e. a 30 mag asteroid contaminates the photometry with 1 percent the flux of a 25 mag star, which is the predicted S/N).

Thus, the SAM needs extending toward small sizes, in the 10 m – 1 km range. For the following simulations, we designed an extension, and added many small asteroids to the SAM. The newly added point sources follows the same celestial distribution as the 1 km-sized asteroids, and they follow the same power slope as does the SAM towards its faint end (power index of -2.75). This power is also consistent with the mean asteroid SDF from Sloan Digital Sky Survey, SDSS hereafter (Parker et al. 2008).

The results of our simulations illustrate how seriously asteroids can contaminate the images toward specific ecliptical directions. In Fig. 1 we plotted the distribution of SAM asteroids in the Solar System at the time of 11 Sep. 2008; Sun and Earth are also marked by yellow and blue symbols. The celestial distribution of the SAM asteroids is plotted in panel B (every 100th asteroids are plotted; the sizes of symbols are scaled to the brightness of the individual objects). Panels C and D show the distribution of objects in our *extended* SAM. Red dots show asteroids that are brighter than 25 mag (which are likely to be detected as point sources in e.g. an average E-ELT image), black dots show objects in the 25–30 mag brightness range. Near the opposition point, at 3.5 degrees latitude, the number of detected asteroids will be $\approx 20,000/\text{sq. degree}$, and 2% of the image area will be contaminated by asteroid trails. In comparison, at 40 degrees elongation from the Sun and at -1.5 degrees ecliptical latitude, 10,000 asteroids/sq. degree will be detected, however, the image area contaminated by asteroid trails will be as large as 10%.

2.1 Confusion noise by undetected asteroids

According to Kiss et al. (2006, 2008), the asteroids must be considered as sources of confusion noise in IR. We summarize this following the cited papers. Near the Ecliptic the effect of asteroids can be comparable to the contribution of Galactic cirrus emission and of the extragalactic background. Assuming that the celestial distribution of asteroids is locally Poisson-like, the F_{lim} fluctuation power and the $\sigma_{lim}(\lambda_i, S_{lim}, \Omega_p)$ confusion noise of undetected asteroids can be written as

$$\delta F_{lim}(\lambda_i, S_{lim}) = \frac{1}{\Omega_c} \sum_{S_i < S_{lim}} S_i^2(\lambda_i),$$

$$\sigma_{lim}(\lambda_i, S_{lim}, \Omega_p) = \left(\Omega_p \delta F_{lim}(\lambda_i, S_{lim}) \right)^{1/2}.$$

Here Ω_c and ω_p are the effective solid angle of the counting cell and the pixel of the instrument, respectively, and S_j is the observed flux of the asteroid at λ_i . The sum runs over all asteroids in the counting cell (See Fig. 2 for illustration). With this technique, Kiss et al. (2006, 2008) presented an all-sky map of the confusion noise by asteroids. Their conclusions were:

- The confusion noise is most significant near the Ecliptic and peaks at the local anti-solar point. Seasonal variations were also detected.
- Mid-infrared surveys like Spitzer/MIPS at 24m and Akari/IRC may be strongly affected by confusion noise in the vicinity of the ecliptic plane.
- 3m-class IR telescopes like Herschel or SPICA will be unaffected. Asteroid confusion would not be negligible in anti-solar direction, however, solar aspect constraints for satellites usually do not allow to observe towards opposition targets.

A confusion noise estimator for several infrared instruments is hosted by the Konkoly observatory ¹. It was prepared to estimate the impact of the asteroids on infrared (IR) and submillimeter observations, from $5\mu\text{m}$ to $1000\mu\text{m}$. The calculations are based on the Statistical Asteroid Model (Tedesco et al. 2005).

The Zodiacal light can be also considered as a possible error source in the infrared. Ábrahám et al. (1997) mapped five $0.5(\text{deg}) \times 0.5(\text{deg})$ fields at low, intermediate and high ecliptic latitude at $25\mu\text{m}$ with the photometer onboard the Infrared Space Observatory. According to their results, no structures were seen in these five sample fields. For an aperture of $3'$ diameter they found an upper limit for the underlying rms brightness fluctuations of $\pm 0.2\%$, that corresponded at high ecliptic latitudes to $\pm 0.04\text{ MJy/sr}$ or $\pm 25\text{mJy}$ in the beam. However, more sensitive instruments may detect the fluctuations of the zodiacal light, and in the future it may show a non-negligible contribution to the far-IR confusion near the ecliptic plane (Maris et al. 2006).

2.2 Contamination by detected asteroids not recognized as asteroids

An asteroid is detected when it is identified as a point source in at least one imaging bandpass. If this happens, automated pipelines tend to add this detection to the list

¹ <http://pc100.konkoly.hu/~apal/sam/>

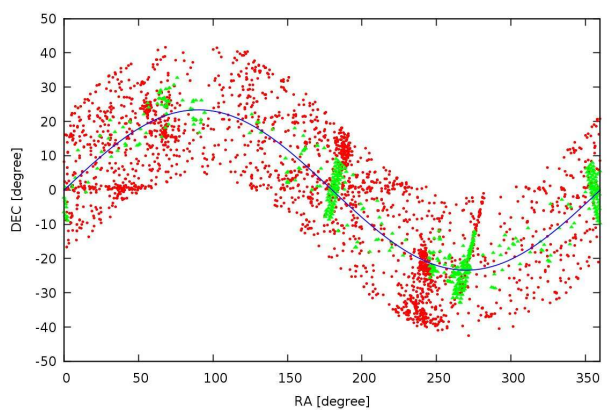


Fig. 3 Area covered by Spitzer MIPS scans (in red) and individual MIPS images (in green) near Ecliptic. All images cover 830 sq. degree in total. We identified 8472 asteroid detections by serendipity in these images.

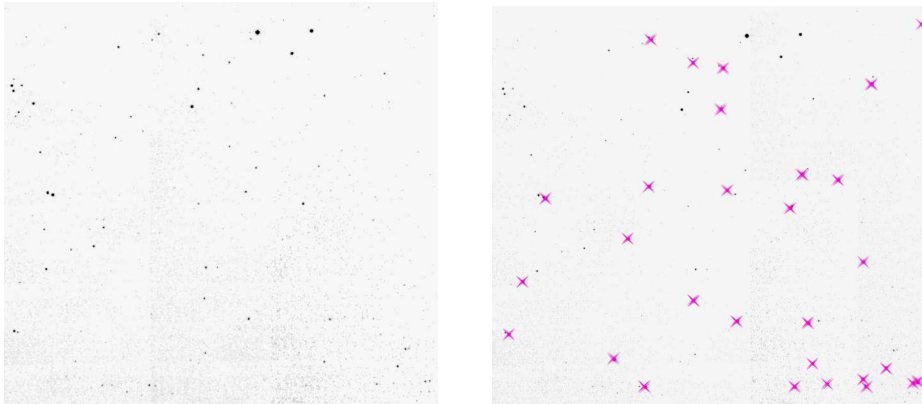


Fig. 4 Detections of asteroid in a sample Spitzer image (showing an area in Taurus, Prop. num. 30816, P.I. Deborah Padgett) by serendipity. Left panel: a region from the mosaic (300×300 arc minute). Right panel: the same image, but with predicted positions of known asteroids (ephemeris generated by JPL/Horizons system). About 75% of the predicted positions can be linked to a point source detection in the Spitzer image (see details in the text).

of point sources, which can lead to severe consequences. Primarily, these asteroids will contaminate the list of star fields in the visual wavelengths because their photometric colors are near to the solar values. In the infrared, they may contaminate the point sources with excess IR light (post-AGB candidates, debris disk candidates etc.) due to their thermal radiation with temperatures $\approx 100\text{--}250$ K. When the objects move fast enough to produce deblended images in different passbands, it will result in false candidates for objects with nonstellar colors. In particular, the candidate quasars selected for SDSS spectroscopic observations would be significantly contaminated because they are recognized by their nonstellar colors (Ivezić et al. 2001, Richards et al. 2001).

2.2.1 Case Study 1: Serendipitous asteroid detections by Spitzer

To test how many main-belt asteroids can be identified in infrared space survey images serendipitously, we tried to identify the known asteroids in selected Spitzer images. First, we collected image data for MIPS scans near the Ecliptic. The images covered 830 sq. degrees in total (Fig. 3). Then we configured `xephemdb`² to identify the known asteroids in (and in the close neighborhood of) these fields. While `xephemdb` does not take all perturbations into account, we uploaded the list of candidate detections to the JPL Horizons Ephemeris Generator³ and extracted the coordinates for the time of observation. Finally we marked these positions onto the images (Fig. 4).

In total, we got a list of 8472 objects in 830 sq. degree sky area, that is ≈ 10 candidate asteroid detections/sq. degree. Most of these asteroids can indeed be identified in Spitzer images as point sources. Half of the detected asteroids can be found within a pixel to the predicted position. About 50% of them is 3-4 arc seconds off, mostly because the orbits of these asteroids are not well known. Despite of this difference in position, the identification looks to be certain for most of the objects. 20% of the detected objects is an entry in the SDSS Moving Object Catalog, and cross-linking the data will result in an optical-infrared multi-wavelength catalog for more than 1500 asteroids.

Our prediction is that Spitzer will finally make ≈ 80 –100 thousand detections of known asteroids and the majority of them will have an optical counterpart in SDSS Moving Object Catalog (MOC). These data will give key information about the structure of the asteroid belt, the formation and evolution of our Solar System and extrasolar systems, too (e.g. Hines et al. 2007, Ryan et al 2008, Bhattacharya et al. 2008, Barucci et al. 2008, Lamy et al. 2008 etc.). The first results of SDSS MOC show the power of survey approach in Solar System studies (see e.g.: asteroid SDF and fine structure of families: Ivezić et al. 2002, Parker et al. 2008; albedo variegation on asteroids: Szabó et al. 2004; space weathering as family age indicator: Nesvorný et al. 2005; evolution of the shapes to less elongated forms in 1-2 billion years: Szabó and Kiss, 2008; distribution of Trojan asteroids Szabó et al. 2008, Trojan subfamilies: Roig et al. 2008).

A serious limit of Spitzer images is that post Basic Calibrated Data (post-BCD) images cannot be used for asteroid photometry, mainly because the image combination process more or less eliminates the moving objects from the results (Z. Balog, personal communication). The other problem is the poor fit of predicted and measured astrometric positions at least in a considerable fraction of cases (also noted by Trilling et al. 2008). Therefore, the recognition and extraction of all serendipitously observed asteroids require special algorithms, and also better known orbits. Asteroid detections by Pan-STARRS will lead to precise orbit elements for most of Spitzer asteroids, which will allow the precise calculation of the ephemerides. It is likely that a full Spitzer asteroid catalog of ≈ 100 thousand detections can be released in the post-Pan-STARRS era. Concerning the Herschel observatory, we can predict a similar number of asteroid detections by serendipity in the MID-IR images (however, the numbers highly depend on the fraction of MID-IR observations, which is likely to be low in the favor of FAR-IR observations).

² <http://www.clearskyinstitute.com/xephem>

³ <http://ssd.jpl.nasa.gov/?horizons>

2.2.2 Case Study 2: Asteroid Confusions at ELTs

The problems with asteroid confusion occur differently with ELTs. The field of view of typical E-ELT instruments will be of the order of 1 sq arcmin, maybe less. Furthermore, E-ELTs will likely work in the IR only since they intend to reach diffraction limit (which is of the order of 25 marcs for a 25m telescope). A surface density of 20000 asteroids/sdeg compares to about 5 asteroids per typical field of view. Certainly, trailing of the asteroid images will be of concern, however, this number of asteroid detections will not be a serious source of error.

One can ask whether TNOs contaminate the images. The complete answer is difficult while we even do not know the number and size distribution of TNOs. Kiss et al (2008) examined this question for a single TNO object and compared its infrared flux to a similarly large main-belt asteroid. While TNOs are ≈ 10 times farther from the Sun than MB asteroids, their black body equilibrium temperature is $\sqrt{10}$ times less. (The surface temperature is even lower when the asteroid has large optical albedo.) Consequently, the IR radiation power is 10^2 less for a TNO than for a similar MB object, which leads to a 10^4 less flux density through the Lambert-law. Because of this factor, the TNOs do not seem to be severe sources of confusion.

Interestingly, TNOs may somewhat deteriorate the fast photometric series of point sources by their occultations. Because of diffraction effects the point sources do not disappear during the event, the occultation means a slight diminishment of the background object up to 50% of the optical flux. This takes for $< \approx 50$ ms, and was observed for several times by Georgevits (2006) and Roques et al (2008). The observed probability of one such event is in the order of $< \approx 1\%$ per night for a single star at low ecliptic latitudes.

3 Asteroid data bases – potentials with extremely large telescopes

We conclude that asteroid detection and identification is a necessary step in reducing data from large telescopes, especially those ones which work (also) in survey mode with highly automated pipelines. The presence of the undetected and/or unidentified asteroids is a considerable error source for many kind of observation (mostly those ones that utilize photometry of point sources, surface photometry and stellar statistics). The solution is to detect as many asteroids as possible. In Solar System science, this eliminated contamination will result in huge catalogs containing multicolor photometry of asteroids. Moreover, catalogs from different sky surveys can be linked to each other, resulting in a multiwavelength spectral albedo distribution of hundred thousands of asteroids. These data will finally provide basic information about asteroids, e.g. their size and albedo distributions, distribution of shape elongations, and also detailed shape models, and finally will give a deep insight into the origin and evolution of the Solar System.

Because asteroid confusion predictions are model-dependent, the limitations of a statistical asteroid model (e.g. SAM) propagate to the predictions based on this model. In SAM, the SDF of asteroid is unique independently of their other properties such as the orbital elements. Most recently, SDF has been recognized to vary significantly in different families, and being different from size distributions for background populations. The families also have sub-structure: the cores tend to host a larger fraction of large asteroids. In old families, a well-defined change of slope is shown that can

be modeled as a broken power-law (Parker et al. 2008). Collisional evolution models predict very steep SDF for the small fragments in certain asteroid families (Michel et al. 2004). The SAM does not take the small (<1 km) asteroids into account. One can extrapolate an existing model (e.g. SAM) toward small sizes (just like we did in this paper), but may be that the SDF slope varies in that size range and the results will be misleading. These recently recognized SDF structures alert that all models which intend to describe the SDF of all asteroids in the Solar System needs to be updated.

The conclusion is that new statistical asteroid models are urgently needed for more precise predictions. The optimal model must be complete to at least the >100 m size range, while the SDF of different families and of the background should be adjusted separately. However, this composition requires a large set of variables (thermal properties, spectral albedo distributions and position-dependent SDFs for all the included families and the background) which by now have not been constrained by observations too well. The infrared space observatories (e.g. Herschel) and the giant Earth-based telescopes (e.g. LSST, E-ELT) will play a key role in building up a statistical asteroid model. This will finally lead us to the better understanding of the asteroid confusions, and not least, to the better understanding of the evolution of the Solar System.

Acknowledgements This work has been supported by the Bolyai János Research Fellowship of the Hungarian Academy of Sciences and the Hungarian OTKA Grant K 76816. The traveling and living expenses were financed by the National Office for Research and Technology, Hungary (Mecenatura Grant) and a funding provided by the LOC. We thank Attila Moór for his kind help. ITM Dr. J. U.

References

1. Ábrahám, P., Leinert, Ch., Lemke, D., 1997, *A&A*, 328, 702
2. Barucci, M. A et al., 2008, *A&A*, 477, 655
3. Bhattacharya, B., Mueller, T. G., Kaasalainen, M., 2008, *LPICo*, 1405, 8311
4. Georgevits, G., 2006, *DPS*, 38, 3707
5. Hines, D. C. et al., 2007, *Bul. AAS*, 39, 751
6. Ivezić, Ž. et al., 2001, *AJ*, 122, 2749
7. Ivezić Ž. et al., 2002
8. Kiss, Cs., Pál, A., Müller, Th., Ábrahám, P., 2008, *A&A*, 478, 605
9. Kiss, Cs., Pál, A., Müller, Th., Ábrahám, P., 2006, *PADEU*, 17, 135
10. Lamy, P. L. et al., 2008, *A&A*, 487, 1187
11. Maris, M., Burigana, C., Fogliani, S., 2006, *A&A*, 452, 685
12. Meadows, V.S., Bhattacharya, B., Reach, W.T. et al., 2004, *ApJS* 154, 469
13. Michel, P., Benz, W., Richardson, D. C., 2004, *P&SS*, 52, 1109
14. Nesvorný, D., Jedicke, R., Whiteley, R. J., Ivezić, Ž., 2005, *Icarus*, 173, 132
15. Parker, A., Ivezić, Ž., Jurić, M., Lupton, R., Sekora, M. D., Kowalski, A., 2008, *Icarus*, 198, 138
16. Roques, F., Georgevits, G., Doressoundiram, A., 2008, in: *The Solar System Beyond Neptune*, M. A. Barucci, H. Boehnhardt, D. P. Cruikshank, and A. Morbidelli (eds.), University of Arizona Press, Tucson, 545
17. Ryan, E. L., Carey, S., Mizuno, D., Woodward, C., 2008, *Bul. AAS*, 40, 193
18. Richards, G. T., et al. 2001, *AJ*, 121, 2308
19. Szabó, Gy.M., Ivezić Ž., Jurić M., Lupton R., Kiss, L. L., 2004, *MNRAS*, 348, 987
20. Szabó, Gy.M., Ivezić Ž., Lupton R., Jurić M., 2007, *MNRAS*, 377, 1393
21. Szabó, Gy. M., Kiss, L. L., 2008, *Icarus*, 196, 135
22. Tedesco et al., 2005, *AJ*, 129, 2869
23. Tedesco, E.F., Désert, F.-X., 2002, *AJ* 123, 2070